Optik - International Journal for Light and Electron Optics 182 (2019) 139–143

Contents lists available at ScienceDirect

Optik

journal homepage: www.elsevier.com/locate/ijleo

Short note

InGaAs/GaAsP strain quantum well spatial light modulator with low voltage and high contrast ratio☆

Yaobiao Li[a], Youwen Huang[a,b,*], Yongqiang Ning[a,b], Lijun Wang[a,b]

[a] Changchun Institute of Optics, Fine Mechanics and Physics, Chinese Academy of Sciences, Changchun 130033, China
[b] State Key Laboratory of Luminescence and Applications, Changchun Institute of Optics, Fine Mechanics and Physics, Chinese Academy of Sciences, Changchun 130033, China

ARTICLE INFO

Keywords:
Spatial light modulator (SLM)
Asymmetric Fabry-Perot cavity
Multiple-quantum wells
Electro-optical device
Optical communication

ABSTRACT

We report a spatial light modulator (SLM) which consisted of 40 pairs of InGaAs/GaAs/GaAsP multiple-quantum wells (MQWs) that embedded in an asymmetric Fabry-Perot (FP) cavity formed by highly reflective back distributed Bragg reflectors (DBRs) and moderate reflective top DBRs. The center wavelength of FP cavity was designed to have a 20 nm redshift in comparison to the luminescence peaks of MQWs. The relationship between optical absorption spectrum of MQWs and the applied negative voltages was modeled based on the quantum-confined stark effect (QCSE). Large area SLMs with 3 mm diameter were fabricated, which exhibited a high contrast ratio of 12:1 at ≃940 nm with only 2 V bias. The QCSE effect varying with the applied voltage and the cavity resonant wavelength shifting with the incident angle were also analyzed theoretically and experimentally. The device is promising to improve system performance and reduce power consumption of fast emerging high-speed data transmission within data centers and short board to board interconnects.

1. Introduction

The spatial light modulator (SLM) is operated based on the quantum-confined stark effect (QCSE), which describes the energy gap change with the application of an external electric field [1]. The SLMs have the advantage of a comparatively low driving voltage, a high speed, and a large contrast ratio between a turn-on state and a turn-off state to be a natural choice in optical links such as 3D imaging applications [2–4], fiber-to-the-home applications [5] optical switch [6], free-space optical communication [7], optical computing and optical correlators [8]. The SLM is also a key element for free-space optical (FSO) communications [9,10], which are knew as optical wireless communication or laser communication between 850 nm and 1550 nm.

Many efforts have been made to improve its performance. To decrease the operation voltage, a coupled quantum wells (CQW) electro-absorption modulators with enhanced absorption change at 1550 nm, which exhibited contrast ratios of 4:1 (6 dB) at a 12 V driving voltage was demonstrated [11]. A stepped quantum well structures operating at 1550 nm with low insertion loss that shows a 7 dB higher extinction ratio compared with coupled quantum well devices were presented by the NU in USA [12,13]. To improve the

☆ Supported by the National Key Research and Development Program (2016YFE0126800); National Natural Science Foundation of China (61434005, 61474118, 11774343, 11674314, 61727822 and 11504370); the Science and Technology Program of Jilin Province, China (20150203011GX); the Science and Technology Program of Changchun City, China (15SS02), and the Youth Innovation Promotion Association of China (2017260).

* Corresponding author at: Changchun Institute of Optics, Fine Mechanics and Physics, Chinese Academy of Sciences, Changchun 130033, China.
E-mail address: huangyouwen13@mails.ucas.ac.cn (Y. Huang).

https://doi.org/10.1016/j.ijleo.2018.12.123
Received 5 December 2018; Accepted 23 December 2018

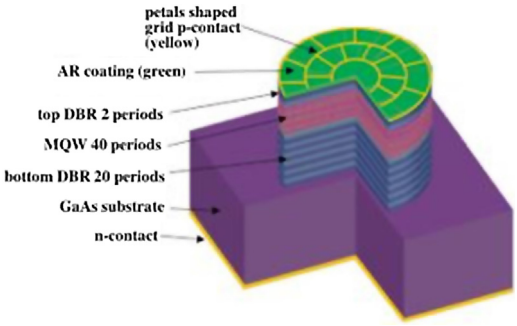

Fig. 1. Schematics of SLM.

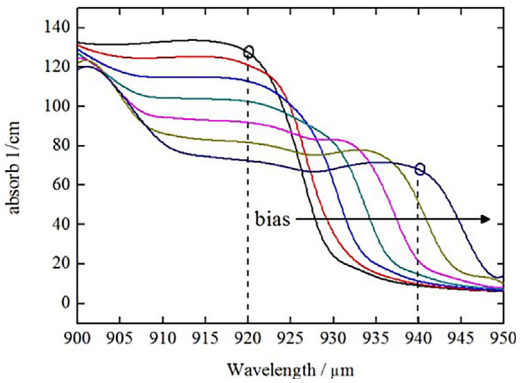

Fig. 2. Calculated optical absorption at 0 to 6 volt biases with step 1 volt.

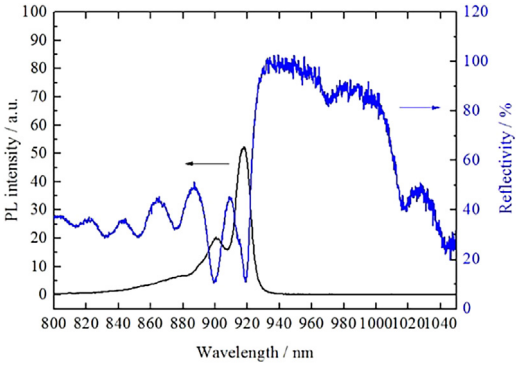

Fig. 3. PL spectrum and reflective spectrum of this grown SLM. The luminescence peaks were at 920 nm.

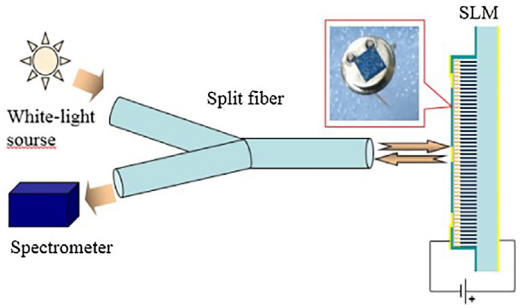

Fig. 4. The measurement setup of SLM.

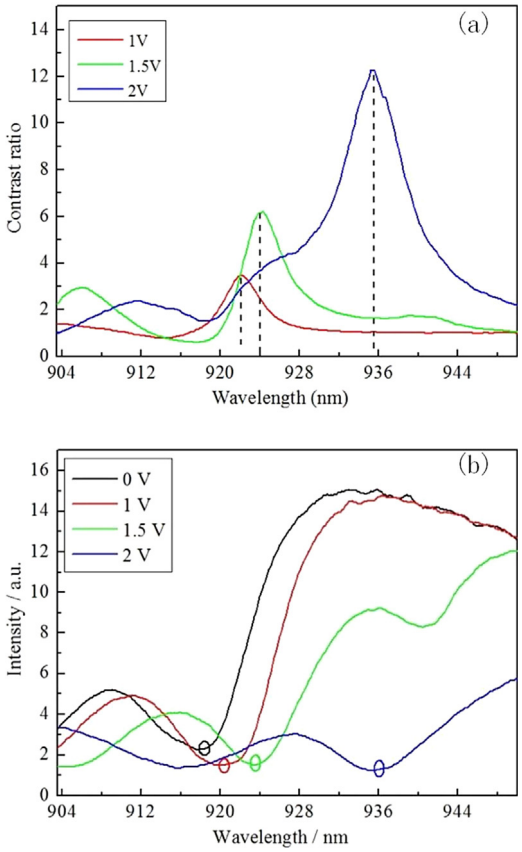

Fig. 5. (a) The modulated reflective spectra of the SLM at room temperature with various reverse biased voltages. The shifting and the broaden of the absorption peaks induced by the QCSE were demonstrated clearly. (b) The corresponding Contrast ratio of the SLM.

contrast ratio of MQW modulator, utilizing optical cavities such as Asymmetric Fabry Perot (ASFP) modulators was firstly proposed to present a contrast ratio of 8:1 at a drive voltage of 50 V in 1994 [5]. A light modulator array was made by Israel Lenslet company to achieve a contrast ratio of 100:1 under 4 V at 846 nm [14]. 1.5 × 1.5 cm^2 devices exhibit contrast ratio of 8 dB at a driving voltage of 8 V and a modulation frequency higher than 10 MHz by a pixelated approach was fabricated by Q. Wang et al. in Sweden [15]. A novel tensile-strained asymmetric quantum-well absorption layer was to obtain a small-chirp operation and a high extinction ratio over 11 dB simultaneously was proposed by Y Miyazaki et al. in Japan [16].

Recently, laser transceiver and optical interconnection based on 940 nm were gaining more and more attention in the field of fast emerging high speed data transmission within data centers and short board to board interconnects [17]. Here we present the design and fabrication of a InGaAs/GaAsP MQW modulator for 940 nm with contrast ratio 12:1 (10 dB) under a low voltage 2 V.

2. Design and simulation

As depicted in Fig. 1, the structure for the SLM consisted of top distributed Bragg reflectors (2 pairs of AlGaAs/GaAs DBRs, giving a wide reflection bandwidth), active layer (40 pairs of InGaAs/GaAs/GaAsP quantum well), p-doped and n-doped contact layers, bottom DBRs (20 pairs of GaAs/AlGaAs designed as a high reflector mirror) and 200 μm GaAs substrate.

In order to obtain acceptable contrast ratios and low voltage swings, we developed a surface normal reflective type modulator based on InGaAs/GaAsP MQWs for an operating wavelength near 940 nm in this work. To achieve the desired spectrum response, commonly, a large number of quantum-well stacks need to be deposited which inevitably introduce dislocations or atomic defects at the heterointerfaces. So a 2 nm GaAs interlayers was inserted between wells and barriers to further prevent lattice relaxation during the process of epitaxial growth and achieve better crystal quality [18]. The monolayer of strain-neutral GaAs interlayers enhanced the carrier transport [19] and made the heterointerfaces smoother so that the subsequent layers could be more easily grown. A $\lambda/4n$ thick silicon-oxide passivation layer was designed to serve as an antireflection (AR) coating here. In SLM, the switch speed can be limited by the high device capacitance defined by the area size of the modulators active. In order to lower the large capacitance of the devices and the high sheet resistance of the p-doped electrode layer. The petals shaped grid p-electrode was formed on top of p-doped contact layer to reduce the effective resistance that shown in Fig. 1 right. It can help increase the modulation rate and achieve uniform frequency response over a large area [20–22].

The relationship of optical absorption spectrum versus the negative applied voltages by this designed structure was calculated by

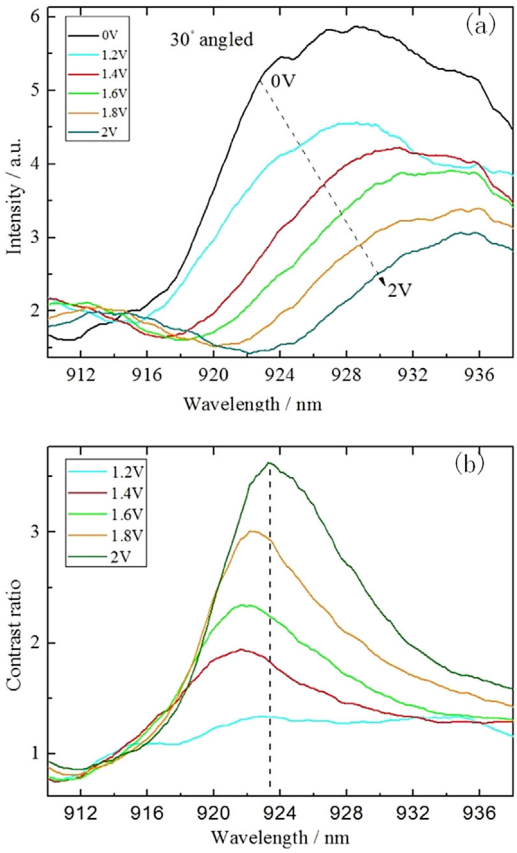

Fig. 6. (a) The modulated reflective spectra of 30 °C incident light under different DC voltage. (b) The contrast ratio under different DC bias.

combining the 3D finite element photonic device simulation software Crosslight and the transfer matrix method, and the results were shown in Fig. 2. It was obtained after calculating the Eigen energy states by solving the Schrodinger equation with appropriate boundary conditions [3]. The incident beam was assumed as 920 nm to adjust the response wavelength of 940 nm when bias voltage was set. When the DC negative voltage applied from 0 V to 6 V, the absorption edge moves towards longer wavelength and the maximum absorption is reduced, that satisfy the QCSE effect.

3. Results and discussion

The epitaxy structure of the MQW modulator was grown by metal-organic chemical vapor deposition (MOCVD) on the (100) GaAs substrate. The photoluminescence (PL) spectroscopy and reflective spectrum was shown in Fig. 3.

The modulation characteristic of the SLM was measured through the built in Fig. 4. A white light source (300–1200 nm) was delivered to the device through a split fiber. The illuminating light penetrated into the device, and the modulated light reflected from the device was coupled into the optical fiber and detected by an optical spectrum analyzer. The bias was applied to the SLM through the pins of the TO package.

The maximum reflective intensity peaks of the SLM had a redshift and a decrease when the backward bias increased from 0 V to 2 V, as shown in Fig. 5(a). The QCSE was considered to cause the obvious change in reflective spectra. The maximum contrast ratio of 12:1 (10 dB) was achieved at backward bias 2 V, and the absorption peak located as 936 nm, as shown in Fig. 5(b).

To test and verify the angled sensibility of the SLM, the modulated reflective spectra for increasing direct voltage with the incidence angle of 30 °C was also measured and shown in Fig. 6. When the increasing dc bias applied on the SLM, the best modulation wavelength varied from 936 nm in Fig. 5 to 924 nm in Fig. 6. Accordingly, the contrast decreased to 3.6:1 at the 30 °C incident angle at 2 V. Nevertheless, it can meet the fundamental requirement contrast ratio of 2:1 in most applications mentioned above.

4. Conclusion

A SLM with InGaAs/GaAsP MQWs for operating at 940 nm is demonstrated in this work. A maximum contrast ratio of 12:1 under voltage of 2 V (less than 5 V) is achieved, which can be driven by standard electronic circuitry. The QCSE effect varying with applied voltage and the cavity resonant wavelength shifting with incident angle are also analyzed theoretically and experimentally in this

work. The specific wavelength modulator may work as an important role for the short reach optical communication and interconnect.

References

[1] S. Junique, Q. Wang, H.H. Martijn, J. Guo, B. Noharet, J. Borglind, B. Hirschauer, H. Malm, D. Agren, O. Oeberg, J.Y. Andersson, Multiple quantum well spatial light modulators: design, fabrication, characterization, Proc. SPIE 4457 (2001) 62–71, https://doi.org/10.1117/12.447739.

[2] S.H. Lee, C.Y. Park, J.-W. You, H. Yoon, Y.-C. Cho, Y.-H. Park, 850 nm IR transmissive electro-absorption modulator using GaAs micromachining, Sens. Actuators A: Phys. 197 (2013) 47–52, https://doi.org/10.1016/j.sna.2013.04.009.

[3] B.H. Na, G.W. Ju, H.J. Choi, Y.C. Cho, Y.H. Park, Y.T. Lee, Large aperture asymmetric Fabry Perot modulator based on asymmetric tandem quantum well for low voltage operation, Opt. Express 20 (2012) 6003–6009, https://doi.org/10.1364/OE.20.006003.

[4] B.H. Na, G.W. Ju, H.J. Choi, S.K. Lee, S. Ravindran, Y.C. Cho, Y.H. Park, C.Y. Park, Y.T. Lee, Coupled tandem cavities based electro-absorption modulator with asymmetric tandem quantum well for high modulation performance at low driving voltage, Opt. Express 21 (2013) 27924–27932, https://doi.org/10.1364/OE.21.027924.

[5] R.N. Pathak, J.E. Cunningham, W.Y. Jan, K.W. Goossen, InGAAs-InP P-I (MQW)-N surface-normal electroabsorption modulators exhibiting better than 8:1 contrast ratio for 1.55 μm applications grown by gas-source MBE, IEEE Photonics Technol. Lett. 6 (1994) 1439–1441, https://doi.org/10.1109/68.392218.

[6] B.H. Na, K.M. Park, R. Sooraj, B.K. Jeong, Y.M. Song, Y.T. Lee, C.-S. Park, Design fabrication and characterization of asymmetric Fabry Perot modulator for large size optical shutter, Opt. Quantum Electron. 19 (2009) 513–517, https://doi.org/10.1109/ICIPRM.1995.522246.

[7] W.S. Rabinovich, 45-Mbit/s cat's-eye modulating retroreflectors, Opt. Eng. 46 (2007) 104001–104008, https://doi.org/10.1117/1.2789634.

[8] B. Zeng, Z. Huang, A. Singh, Y. Yao, A.K. Azad, A.D. Mohite, A.J. Taylor, D.R. Smith, H.-T. Chen, Hybrid graphene metasurfaces for high-speed mid-infrared light modulation and single-pixel imaging, Light: Sci. Appl. 7 (2018) 1–8, https://doi.org/10.1038/s41377-018-0055-4.

[9] Q. Wang, B. Noharet, S. Junique, S. Almqvist, D. Agren, J.Y. Andersson, 1550 nm transmissive/reflective surface-normal electroabsorption modulator arrays, Electron. Lett. 42 (2018) 47–49, https://doi.org/10.1049/el:20063504.

[10] M. Achour, Free-space optical communication by retro-modulation: concept, technologies and challenges, Proc. SPIE 5614 (2004) 52–63, https://doi.org/10.1117/12.582754.

[11] Q. Wang, 1550 nm surface normal electroabsorption modulators for free space optical communications, Proc. SPIE 5986 (2005) 898610–898617, https://doi.org/10.1117/12.630395.

[12] H. Mohseni, W.K. Chan, H. An, A. Ulmer, D. Capewell, Tunable surface-normal modulators operating near 1550 nm with a high-extinction ratio at high temperatures, IEEE Photonics Technol. Lett. 18 (2005) 214–216, https://doi.org/10.1109/LPT.2005.861629.

[13] U. Arad, E. Redmard, M. Shamay, A. Averboukh, S. Levit, U. Efron, Development of a large high-performance 2-d array of GaAs-AlGaAs multiple quantum-well modulators, IEEE Photonics Technol. Lett. 15 (2003) 1531–1533, https://doi.org/10.1109/LPT.2003.818663.

[14] H. Mohseni, W.K. Chan, H. An, D. Capewell, High-performance optical modulators based on stepped quantum wells, Proc. SPIE (2006), https://doi.org/10.1117/12.640530.

[15] Q. Wang, S. Junique, D. Agren, B. Noharet, J.Y. Andersson, Fabry-Perot electroabsorption modulators for high-speed free-space optical communication, IEEE Photonics Technol. Lett. 16 (2004) 1471–1473, https://doi.org/10.1109/LPT.2003.818663.

[16] Y. Miyazaki, H. Tada, S.-y. Tokizaki, K. Takagi, T. Aoyagi, Y. Mitsui, Small-chirp 40-gbps electroabsorption modulator with novel tensile-strained asymmetric quantum-well absorption layer, IEEE J. Quantum Electron. 39 (2003) 813–819, https://doi.org/10.1109/JQE.2003.811593.

[17] A. Melgar, J. Lavrencik, Experimentally benchmarked fiber propagation model for 50Gbps PAM-4 MMF links employing multimode VCSELs, Optical Fiber Communication Conference W3G (2017), https://doi.org/10.1364/OFC.2017.W3G.6 W3G.6.

[18] H. Fujii, Y. Wang, K. Watanabe, M. Sugiyama, Y. Nakano, Suppressed lattice relaxation during InGaAs/GaAsP MQW growth with InGaAs and GaAs ultra-thin interlayers, J. Cryst. Growth 352 (2012) 239–244, https://doi.org/10.1016/j.jcrysgro.2011.11.036.

[19] Y. Wang, Y. Wen, M. Sugiyama, Y. Nakano, InGaAs/GaAsP strain-compensated superlattice solar cell for enhanced spectral response, J. Cryst. Growth (2010) 003383–003385, https://doi.org/10.1109/PVSC.2010.5614127.

[20] P.G. Goetz, W.S. Rabinovich, S.C. Binari, J.A. Mittereder, High-performance chirped electrode design for cat's eye retro-reflector modulators, IEEE Photonics Technol. Lett. 18 (2006) 2278–2280, https://doi.org/10.1109/LPT.2006.884725.

[21] P.G. Goetz, R. Mahon, T.H. Stievater, W.S. Rabinovich, S.C. Binari, High-speed large-area surface-normal multiple quantum well modulators, Proc. SPIE 5160 (2004) 346–354, https://doi.org/10.1117/12.507768.

[22] W.S. Rabinovich, Free-space optical communications link at 1550 nm using multiple-quantum-well modulating retroreflectors in a marine environment, Opt. Eng. 44 (2005), https://doi.org/10.1117/1.1906230 056001–12.